

Explicit Finite Element Analysis of Inflatable Braided Strapped Beams

Jeremy L. Hill¹ and Robert D. Braun²
Georgia Institute of Technology, Atlanta, GA, 30332-0150

Inflatable Aerodynamic Decelerators and other air inflated structures, such as airbeams, quite often utilize woven or braided fabrics due to their lightweight and high loading carrying capabilities. An airbeam is a high-strength fabric sleeve with a highly flexible internal bladder that can be used as a load-bearing beam when inflated. Due to their fabric construction, airbeams are inherently thin walled structures that are prone to local buckling. Design optimization of these inflated structures relies on a detailed understanding of the fabric mechanics. In this study, three-dimensional membrane finite element models were used to predict the beam load–deformation response given experimentally obtained moduli. The finite element models successfully predicted localized fabric buckling and softening of load–deflection response. The finite element model and test results indicate that the consideration of work done by pressure under deformation-induced volume changes may increase beam capacity.

Nomenclature

E = Elastic Modulus
 G = Shear Modulus
 ν = Poisson's Ratio

Subscripts

1 = Longitudinal Direction
 2 = Lateral Direction
 12 = Plane Defined by 1,2 axes

Acronyms

IAD = Inflatable Aerodynamic Decelerator
 FEA = Finite Element Analysis

¹ Graduate Research Assistant, Daniel Guggenheim School of Aerospace Engineering, AIAA Student Member.

² Professor, Daniel Guggenheim School of Aerospace Engineering, AIAA Fellow.

I. Introduction

An airbeam is usually a high strength fabric sleeve fitted around an air retention bladder which, when sealed and inflated, acts as a load bearing structural beam. Depending on how the fabric is woven or braided the members can be shaped in straight or curved sections. Major advantages of airbeams include being lightweight, having low storage volumes and deploying rapidly. Unlike structures fabricated from conventional materials, airbeam structures typically do not experience irreversible damage when over loaded, but will reassume their shape and regain capacity when unloaded. In recent years, inflatable structures have been typically used in space-based applications, recreational tents, and military shelters. An example aerospace application includes Inflatable Aerodynamic Decelerators (IADs) as shown in Fig 1¹. Airbeams date back to the 1950's, but construction methods (seam strengths) limited their use. However, recent advances in textile manufacturing, including 3D weaving and seamless fabric beam construction methods which permit higher operating pressures, have generated new interest in the use of airbeam structures.



Figure 1: NASA's Hypersonic Inflatable Aerodynamic Decelerator¹

An airbeam's load-deflection response is typically linearly elastic until the applied loads produce fabric compressive stresses exceeding the tensile pre-stress caused by inflation pressure, after which the total beam stiffness begins to decrease^{2,3}. This decrease is driven by local buckling or "Wrinkling" of the beam wall, which cannot support much compressive stress. Furthermore, airbeams constructed from woven fabrics have inherently low shear moduli leading to relatively large shear deformations⁴. This can be contrasted with braided fabrics that have inherently low capability to carry axial stresses, but result in relatively low shear deformations.

During the 1960's, Stein and Hedgepeth conducted analytical research into the behavior of inflated isotropic cylindrical membranes. Their work developed mathematical expressions for the beam's load bearing capacity based on a moment-curvature analysis of the post wrinkling response. An important conclusion from their work is that the limit load of an internally pressurized cylindrical membrane beam is twice the wrinkling load of the beam. Fichter used the minimum potential energy principle to develop analytical expressions for the load-deflection response of inflated cylindrical membranes in bending prior to wrinkling⁵. Fichter showed that the increase in inflation pressure caused by deformation induced volume changes of the air, increases the transverse shear rigidity of the airbeam.

Using Euler-Bernoulli beam theory, Veldman developed analytical relationships for the bending of inflated braided airbeams⁶. These expressions worked well in the linear elastic region prior to wrinkling, but required a more empirical approach after wrinkling occurred. Main et al. carried out cantilevered bending tests of inflated Mylar beams with varying length to diameter ratios, as well as, developed analytical solutions for load-deflection response that incorporated the biaxial state of stress in the fabric^{2,3}. Cavallaro et al. found that shear deflections were significant when four point bend tests were conducted on small diameter woven straight airbeams⁷.

A great deal of work has also been done in the development of finite element analysis (FEA) techniques for inflated fabric beams. Wielgosz and Thomas examined the load-deflection response of inflated fabric panels, as well as, developed a beam finite element that included shear deflections and pressure stiffening effects^{8,9,10}. An important

conclusion was that the pressure effectively increases the stiffness properties of an inflated beam. Le van and Wielgosz developed a higher order inflatable beam element that includes pressure stiffening effects¹¹. It was shown that the element predictions of load-deflection, as well as, global buckling of beams and toroidal members agreed well with their prior simulations using membrane theory¹². More recently, Davids et al presents an airbeam finite element that incorporates fabric wrinkling by treating the fabric as a linearly elastic tension-only material¹³. The formulation is based on the principle of virtual work, as well as, incorporating the work done by the internal pressure under deformation induced volume changes due to both shear and bending. Results from the numerical model compared well with the beam four point and three point load-deflection data of Turner¹⁴. Malm et al. used three dimensional membrane finite element models to predict the beam load-deformation response for various elastic and shear moduli¹⁵. The FE models successfully predicted localized fabric buckling and softening of the load-deflection curve.

This paper examines the response of inflatable braided, strapped airbeams both experimentally and numerically. In contrast with most prior studies, an experimental characterization was carried out by the University of Maine of braided airbeam fabric shear constitutive behavior, support strap elastic constitutive properties, and airbeam load-deflection response in bending. In addition, load-deflection behavior in the post wrinkling regime is considered both experimentally and numerically. Braided, strapped fabric airbeams were tested in three and four point bending at several inflation pressures, braid angles, and strap locations. Displacements measured at multiple locations along the span allowed the relative contribution of transverse shear deformations to be quantified. Loads well beyond the theoretical wrinkling load were applied in all cases. The independent determination of the effective fabric shear modulus with a novel tension-torsion test developed by Turner et al is also briefly overviewed¹⁶. Details regarding the development and implementation of a membrane FE model capable of predicting the load-deformation beam response in the pre- and post-wrinkling range are provided. The simulations use an explicit finite element code since it is better suited for modeling transient and unstable phenomena. The model is shown to give good predictions of beam response over a large range of displacements. The FE results indicate that including the work done by pressure due to shear deformation-induced volume changes is important. This work is part of a larger effort to improve simulation techniques and confidence in ground to flight extrapolation of IADs.

II. Experimental Testing

Brayley et al. tested the bending response of inflatable, braided beams and arches with external reinforcing straps¹⁷. The work focused on experimentally determining the constitutive properties of the constituent materials, and quantifying the load-deformation behavior of beams and arches with full scale laboratory tests. The straps were tested in pure tension to obtain accurate tensile modulus. The braided material was tested in torsion to obtain shear modulus as a function of inflation pressure. A beam finite element model that accounts for braid angle and strap stiffness was developed to model the bending response of the inflatable, braided strapped beams and arches. Quasi-static load-deformation tests of arches and beams were performed to provide data for model validation. The FE model effectively predicted the load-deformation in response of the members to and beyond the point of fabric wrinkling.

A. Bend Tests

Inflatable braided, strapped beams were tested at the University of Maine in the 2009. The beams were provided fully assembled by Vertigo, Inc. of Lake Elsinore, CA. The beams were constructed with an internal urethane bladder, a braided fabric at a 75 deg bias, and four external reinforcing straps. The beams were coated for protection from abrasion. Strap material and inflation pressure were varied to determine the effect on the load-deflection response and ultimately obtain load-deflection data for model validation and calibration.

As mentioned above, beams were constructed using two strap types. One strap was much thicker than the other. The exact material was not reported by the authors, but referred to as thin-strapped beam and thick-strapped beam. This paper focuses on the thin reinforcing straps as there was a greater uncertainty associated with the thicker straps. The thin reinforcing straps were approximately 3.175 mm thick and 25.4 mm wide. The four straps were positioned at 65, 115, 245, and 295 deg around the cross section of the beam as seen in Fig 2. Beams were approximately 5 m in length and had a cross-sectional diameter of 262 mm as shown in Table 1.

Table 1. Four Point Bend Configuration Dimensions

Approx. Beam Length (m)	Measured Cross-sectional Diameter (mm)	Support Centerlines (m)	Load Strap Centerlines (m)	Approx. Support Width (mm)	Load Strap Width (mm)	Approx. Strap Width (mm)
5	262	3.75	1.25	200	200	25.4

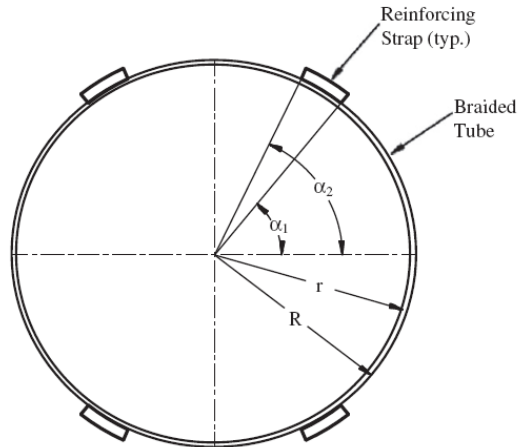


Figure 2: Cross-section of Braided Member with External Reinforcing Straps¹⁷

Tests were conducted at inflation pressures of 69, 138, 207, 276, and 345 kPa. Beams were tested in a three and four point bend configuration; however, this paper focuses on the results from the four point bend tests as shown in Fig 3. The supports consisted of two steel wheels and laminated 2x6 lumber shaped to create a saddle for the beam. This simple support allowed the beam to rotate and move freely. The support frame was constructed to allow the supports to roll freely.

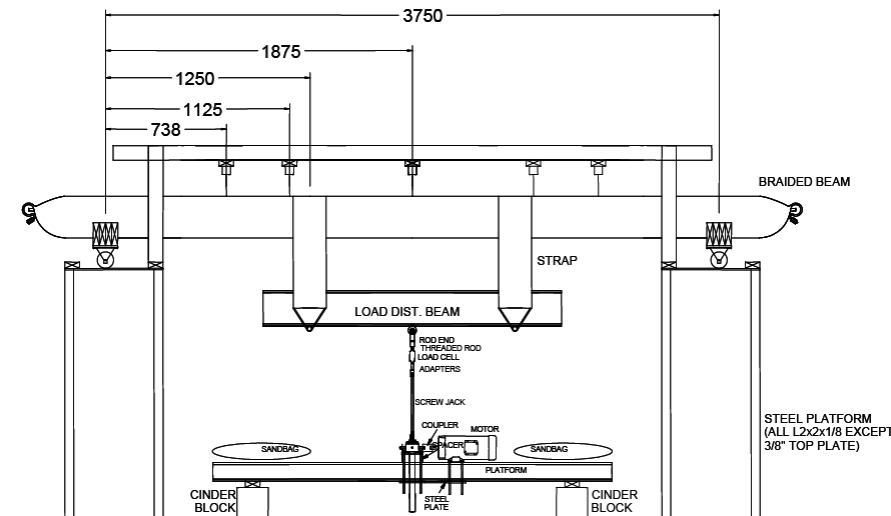


Figure 3: Four Point Bend Test Setup¹⁷

A downward force was applied via an actuator mounted to a platform below the beam. The actuator was attached to a loading beam with a threaded rod. The four point bend test forces were applied at third points on the beam with nylon load straps. To record downward displacements during loading, five string potentiometers were used. The force applied to the beam was measured with a load cell. Inflation pressure was monitored with a pressure sensor placed on the air supply line. The test matrix consisted of the beams being displaced 250 mm in the vertical downward direction three times at each inflation pressure. The 250 mm displacement provided load-deflection response well beyond the initiation of wrinkling.

B. Support Strap Tensile Testing

Tensile tests were performed on samples of uncoated and coated polyester straps at the University of Maine. These straps were used on the inflatable braided, strapped beams. The objectives of this testing were to determine the strap tensile modulus and quantify the effect of strap coating on the tensile modulus. Due to the large role the straps play in the inflatable members bending stiffness, strap stiffness is of particular interest.

The straps tested were 25.4 mm wide, 838 mm long, and cut from virgin material. The uncoated straps consisted of a thick white polyester strap approximately 3.2 mm thick and a thin tan strap that was approximately 0.9 mm thick. As discussed by Brayley, these tests indicated that the coating has virtually zero impact on the strap stiffness¹⁷. For this work, only the uncoated thin strap material is considered for modeling purposes and the thick or coated straps are not discussed further.

The straps were loaded using two split capstan grips. The grips were mounted on an Instron tension-torsion machine. Only the tension capability was utilized. An extensometer with a 50 mm gauge length was placed at the center of the strap to record elongation over the gage length. The test setup is shown below in Fig 4. Brayley notes that while there were no specific test methods for quantifying the stiffness of external reinforcing straps, the following ASTM standards for testing textiles in tension were used: ASTM D 4964-96, ASTM D 1776-08, ASTM D 3822-01, and ASTM D 76-99^{18,19,20,21}.



Figure 4: Tensile Test Setup¹⁷

There were two phases to the testing: a preconditioning phase and a cyclic testing phase. The preconditioning was important as it forced the fibers to pre-align to the direction of the axial load. The straps were loaded to a level similar to that produced during bend tests. Each preconditioning phase was designed to represent the stress levels as seen by the strap at each inflation pressure. There were 7 steps in the loading cycle. The 2nd step represents the stress seen in the strap from just 69 kPa of inflation pressure; and then each step after that represents the stress in the strap corresponding to a 254 mm displacement due to four-point bending and inflation. The last cycle of the preconditioning was repeated until the strap reached a consistent strain. The testing phase consisted of loading the straps to the peak load twenty times.

A strap tensile modulus was calculated using the slope of the loading phase from each of the 20 cycles. The slope of the loading portion of each cycle was calculated using a linear best fit line. The linear range was considered to be the

entire loading range from zero stress to peak stress for all of the straps. An average of the tensile moduli from each of the twenty cycles was taken as the nominal tensile modulus for each strap. The thin strap had a calculated tensile modulus of 35,818 N/mm. Tensile modulus and stress are reported in N/mm due to the strap material being treated as a membrane.

C. Torsion Fabric Testing

Torsion tests were performed on inflatable, braided tubes with coating applied. The purpose was to determine the fabric shear modulus for different braid angles and inflation pressures. It was desired to isolate the material properties of the braided material, so reinforcing straps were not included. The specimens were fabricated with a length of 457 mm, a diameter of 102 mm, and a 75 deg braid angle. The internal bladder was similar that used for the beam testing. As Brayley discusses, due to manufacturing limitations, the braid coverage was approximately 85% of the large beams¹⁷. Thus, the braided torsion specimens are likely more compliant than those used for the beam testing. The two coatings used were a silicone and polyurethane. Three specimens were fabricated with each coating type.

The test setup was originally designed by Turner et al.¹⁴, refined by Kabche et al.¹⁶, and a modified version was used by Brayley¹⁷. The setup used a bi-axial servo-hydraulic Instron testing machine to apply torque. Two aluminum fire house couplings attached to the Instron load cell served as grips as shown in Fig 5. The maximum applied torque was chosen to produce a maximum shear stress corresponding to the expected shear stress in the beam. As discussed in Brayley, the measured torque vs. rotation produced a linear response¹⁷. For further details on the testing and braid property determination, see Brayley¹⁷.



Figure 5: Torsion and Tension Test Setup¹⁷

Table 2 summarizes the shear moduli over the full range of inflation pressures for the polyurethane coated braid. The shear moduli are clearly a function of inflation pressure due to the tow-tow friction and fabric decrimping. The coating has some impact on the response. However, at all inflation pressures, the shear modulus of the braid is at least an order of magnitude larger than that of the plain woven beams tested Turner et al.¹⁴ and Kabche et al.¹⁶. Therefore, the shear deformations of the braided beam are small by comparison.

Table 2. Braid with Polyurethane Coating - Shear Moduli¹⁷

Inflation Pressure (kPa)	G (N/mm)	E (N/mm)
69	210	39
138	263	43
207	304	46
276	339	49
345	369	52

The axial stiffness of the braid was also quantified by Brayley¹⁷, using tensile tests. As expected with braided fabrics, the axial stiffness is very low when compared to the shear stiffness of the tubes and even more so when compared to the axial stiffness of the reinforcing straps (~6% of the strap EA). This is the major justification for assuming that the braid carries only hoop and shear stress.

III. Finite Element Modeling of Airbeam Response

A. Geometric Model Description

LS-DYNA was chosen as the FEA package for this effort, based primarily on its ability to model transient or unstable phenomena²². Four-noded membrane elements were used to model the air beam. The Nylon pull straps and the end caps of the airbeams were modeled with shell elements. Models employed quarter symmetry boundary conditions to minimize computational time. To simulate the linear bearings used in the experiments, a horizontal line of nodes across the diameter of the end cap was allowed to rotate in the plane of beam bending and allowed to translate along the axial direction of the beam. The remaining degrees of freedom for these nodes were fixed. A mesh refinement study was conducted to determine a reasonable element density. Uniform meshes of the cylindrical beams were created with the thin strap location in mind. The final mesh for the four point bend simulations had 6970 total elements and is shown in Fig 6.



Figure 6: CAD model for Four-point Bend Test Simulations

Inflation pressure was applied as a constant surface pressure, with the orientation of the load remaining normal to the surface of each element as the airbeam deflected. Contact between the pull-strap and the airbeam was treated as a “hard” contact with no penetration allowed and zero friction. Self-contact of the airbeam was also included. The analysis was performed in two steps, where the airbeam was first inflated and then the load strap was displaced, deflecting the airbeam to the desired magnitude. The total simulation time was set to 0.4 sec. The inflation pressure gradually ramped up to full pressure over the first 0.1 sec. The load strap was displaced downward to 200 mm over the next 0.1 sec. The oscillations in the model were allowed to damp out over the next 0.2 sec. The displacement of the airbeam at the location of the midspan potentiometer was recorded along with the resultant contact forces between the strap and the beam.

B. Material Model Properties

A linearly elastic orthotropic material model (MAT FABRIC) was used, allowing the user to directly input two orthotropic elastic moduli (E_1 and E_2), the in-plane shear modulus (G_{12}), and the in-plane Poisson’s ratio (ν_{12}). Poisson’s ratio was assumed to be 0.3. The two orthotropic elastic moduli were assumed to be equal, and were taken as the constant value determined from the tensile test. The in-plane shear moduli were taken as the pressure dependent values listed in Table 2.

For comparison with the experimental data found in Brayley, the polyurethane coated braided fabric properties at 3 different inflation pressures were selected¹⁷. For a set inflation pressure, the same fabric material properties were used across the entire beam. The elastic modulus was set using the experimentally obtained values for the uncoated thin strap. The shear modulus was set using the experimentally obtained values for the coated braided tubes. An example input card for the 207 kPa load case is shown in Table 3.

Table 3. LS-DYNA Keyword Parameters for Fabric

*MAT_FABRIC_TITLE

Vectran Braided Beam with Polyurethane Coating (207kPa)

\$#	mid	ro	ea	eb	ec	prba	prca	prcb
	1	1.4e-6	3.582e+10	3.582e+10	0	0.3	0	0
\$#	gab	gbc	gca	cse	el	prl	lratio	damp
	3.04e+8	0	0	1	0	0	0	1

The airbeam had a nominal diameter of 262 mm. Brayley notes that the diameter varied between 261 & 263 mm. To ensure that the inflated diameter was accurately captured by the FEA model, the diameter was checked after inflation. The diameter increased by ~0.1% and therefore still within the range measured by Brayley¹⁷.

C. Model Results & Comparison with Experiments

Fig 7 shows the four point bend experimental results and FEA predictions. The predictions correlate well to the experimental data in the linear elastic range for all three inflation pressures. Post-wrinkling behavior trends well with the experimental data, but at a given load is over predicting the experimental displacements. This may indicate that the FEA models are not adequately capturing the work done by pressure due to deformation induced volume changes in the post-wrinkling regime. The solid markers in Fig 7 signify the theoretical wrinkling loads.

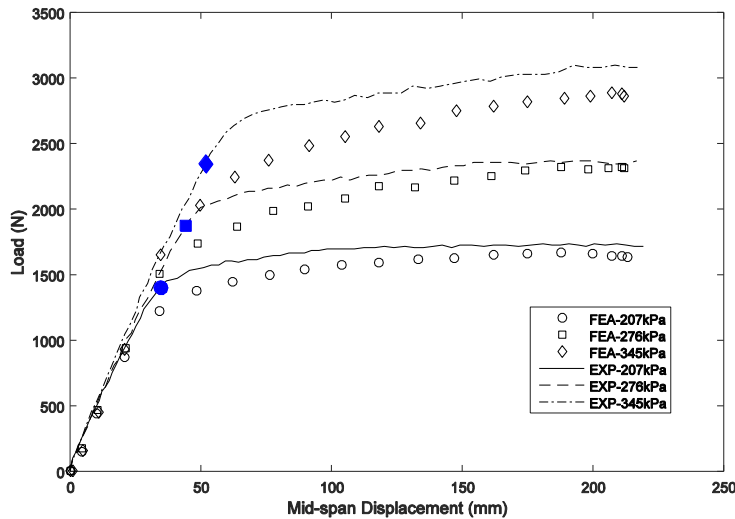


Figure 7: Four Point Bend FE Model Results

IV. Summary and Conclusions

An experimental study on the load-deflection response of inflatable braided, strapped beams was completed by the University of Maine. An FEA study on the same beams was presented in this work. The University of Maine conducted three and four point bend tests of a single inflated fabric beam to assess the load-deflection response, tension-torsion tests were run to measure fabric shear and elastic moduli, and uniaxial loading tests were run to measure the elastic modulus of the support straps. Three dimensional FEA models were constructed with membrane elements to model the beam response using material properties derived independently from the tension-torsion and uniaxial tests.

The results of this study show that finite element modeling of the inflatable braided, strapped airbeams including the effects of internal pressure and local buckling can be accomplished with three dimensional membrane FE models developed with commercially available codes. The relatively large magnitude of shear deformations of the beams

tested by the University of Maine indicates that it is important to increase the effective shear modulus of the fabric to account for the work done by internal pressure as derived by Fichter⁵. The models predicted the onset of fabric wrinkling, and the resulting softening in load-deformation response. Simulations were run using an explicit finite element code, since explicit codes are better suited for modeling transient or unstable phenomena.

Model run times were significant, exceeding a several hours for most simulations on a PC-based workstation. Future numerical simulations will benefit from running simulations across multiple clusters. In addition, future modeling efforts using membrane or shell models should investigate the explicit simulation of the confined, pressurized air as a discrete component to rigorously capture the effect of work done by pressure under deformation-induced volume changes. Finally, the good agreement between the three-dimensional FEA models and experimental four point bend test results indicates that the tension-torsion test method is appropriate for obtaining beam material properties and the development of a computationally efficient method for determining those properties numerically will be useful for the design of inflated fabric beams.

With the use of external reinforcing straps comes the ability to optimize the braid angle to increase operating pressures without the design considerations involving axial stiffness of the braided membrane. When considering the topic of optimal design one must consider fabric material and braid angle along with strap location and strap material. Future modeling efforts should be directed toward capturing the effect of braid angle on load-deflection response.

Acknowledgments

The author would like to thank Dr. William Davids of the University of Maine for sharing information regarding the experimental test data used as validation in this work.

References

- ¹Cassell, A.M., Swanson, G.T., Johnson, R.K., Hughes, S.J., and Cheatwood, F.M.. "Overview of the Hypersonic Inflatable Aerodynamic Decelerator Large Article Ground Test Campaign," 21st AIAA Aerodynamic Decelerator Systems Technology Conference and Seminar, May, 2011
- ²Main JA, Peterson SW, Strauss AM. Beam-type bending of space-based inflated membrane structures. *J Aeros Eng* 1995;8(2):120–5.
- ³Main JA, Peterson SW, Strauss AM. Load–deflection behavior of space-based inflatable fabric beams. *J Aeros Eng* 1994;7(2):225–38.
- ⁴Sun H, Pan N, Postle R. On the Poisson's ratios of a woven fabric. *Comp Struct* 2005;68(4):505–10.
- ⁵Fichter WB. A Theory for inflated thin-wall cylindrical beams. NASA technical note D-3466. Langley Research Center, Langley, Virginia, USA; 1966.
- ⁶Veldman SL, Bergsma OK, Beukers A, Drechlsler K. Bending and optimization of an inflated braided beam. *Thin-Wall Struct* 2005;43:1338–54.
- ⁷Cavallaro PV, Johnson ME, Sadegh AM. Mechanics of pressurized plain-woven fabrics for inflated structures. *Comp Struct* 2003;61:375–93.
- ⁸Wielgosz C, Thomas J-C. Deflections of inflatable fabric panels at high pressure. *Thin-Wall Struct* 2002;40:523–36.
- ⁹Wielgosz C, Thomas J-C. An inflatable fabric beam finite element. *Commun Numer Methods Eng* 2003;19:307–12.
- ¹⁰Thomas J-C, Wielgosz C. Deflections of highly inflated fabric tubes. *Thin-Wall Struct* 2004;42:1049–66.
- ¹¹Le van A, Wielgosz C. Finite element formulation for inflatable fabric beams. *Thin-Wall Struct* 2007;45:221–36.
- ¹²Le van A, Wielgosz C. Bending and buckling of inflated fabric beams: some new theoretical results. *Thin-Wall Struct* 2005;43:1166–87.
- ¹³Davids WG, Zhang H, Turner A, Peterson M. Beam finite element analysis of pressurized fabric tubes. *J Struct Eng* 2007;133(7):990–8.
- ¹⁴Turner AW. Experimental test methods for inflatable fabric beams. MS thesis, Orono (ME): University of Maine; 2006.
- ¹⁵Malm CG, Davids WG, Peterson ML, Turner AW. Experimental characterization and finite element analysis of inflated fabric beams. *Constr Build Mater* 2009;23(5):2027–34.
- ¹⁶Turner AM, Kabche JP, Peterson ML, Davids WG. Tension/torsion testing of inflatable fabric tubes. *Exp Techniques* 2008;32(2):47–52.
- ¹⁷Brayley K. Structural behavior of externally reinforced inflated fabric arches and beams, MS thesis. University of Maine, Orono, ME; 2011.
- ¹⁸ASTM D4964-96. Standard test method for tension and elongation of elastic fabrics (constant-rate-of-extension type tensile testing machine). ASTM International; 2004.
- ¹⁹ASTM D1776-08. Standard practice for conditioning and testing textiles. ASTM International; 2009.
- ²⁰ASTM D3822-01. Standard test method for tensile properties of single textile fibers. ASTM International; 2001.
- ²¹ASTM D76-79. Standard specification for tensile testing machines for textiles. ASTM International; 2005.
- ²²LS-DYNA Keyword User's Manual, Version R8.0, Vol I-II, March 2015.